LAWRENCE
LIVERMORE
NATIONAL
LABORATORY

LLNL-JRNL-701302

Isotopic Fractionation of Oxygen and Carbon in Decomposed Lower-mantle Inclusions in Diamond

F. Kaminsky, J. Matzel, B. Jacobsen, I. D. Hutcheon, R. Wirth

August 24, 2016

Contributions to Mineralogy and Petrology

Disclaimer

LLNL-JRNL-701302

Isotopic fractionation of oxygen and carbon in decomposed lower-mantle inclusions in diamond

Felix Kaminsky[1], Jennifer Matzel[2], Ben Jacobsen[2], Ian Hutcheon[2], and Richard Wirth[3]

[1]KM Diamond Exploration Ltd., 2446 Shadbolt Lane, West Vancouver, BC V7S 3J1, Canada

[2]Lawrence Livermore National Laboratory, 7000 East Avenue, Livermore, CA 94550, USA

[3]Department of Chemistry and Physics of Earth Materials, GeoForschungsZentrum Potsdam, D14473 Potsdam, Germany

Abstract

Two carbonatitic mineral assemblages, calcite + wollastonite and calcite + monticellite, which are encapsulated in two diamond grains from the Rio Soriso basin in the Juina area, Mato Grosso State, Brazil, were studied utilizing the NanoSIMS technique. The assemblages were formed as the result of the decomposition of the lower-mantle assemblage calcite + CaSi-perovskite + volatile during the course of the diamond ascent under pressure conditions from 15 to less than 0.8 GPa. The oxygen and carbon isotopic compositions of the studied minerals are inhomogeneous. They fractionated during the process of the decomposition of primary minerals to very varying values: $\delta^{18}O$ from −3.3 to +15.4‰ SMOW and $\delta^{13}C$ from −2.8 to +9.3‰ VPDB. These values significantly extend the mantle values for these elements in both isotopically-light and isotopically-heavy areas.

Introduction

Over the last two decades, the mineralogical composition of the Earth's lower mantle has become known from mineral inclusions in diamond (e.g., Harte, 2010; Kaminsky, 2012; Harte and Hudson, 2013 and references therein). However, the isotopic characteristics of lower-mantle mineral associations have been poorly studied to date. Only two ion microprobe analyses from a grain of CaSi-perovskite within lower-mantle diamond have been performed; they have yielded values of $\delta^{18}O$ at 4.92 and 6.95‰ SMOW (Harte et al., 1999). The former is close to the average mantle value, while the latter is shifted in the supracrustal values.

Our knowledge of isotopic "average mantle values" of carbon and oxygen is mainly based on, and can be applied to, only the upper-mantle reservoir. The high-precision determination of the upper-mantle oxygen isotopic composition yielded the average value of $\delta^{18}O$ = 5.3±0.6‰SMOW (Valley et al. 1998; Spetsius et al. 2008; Wang et al. 2011; Kostrovitskii et al., 2012; Giuliani et al., 2014). The range of the upper-mantle carbon isotopic composition is from −2 to −8‰ $\delta^{13}C$ VPDB, while for the lower mantle the range is suggested to be wider, from −0.5 to −8.5‰ $\delta^{13}C$ (Cartigny, 2005). A detailed study of lower-mantle diamonds from Juina (Brazil) and Kankan (Guinea) confirmed the similarity of the lower-mantle and the upper-mantle carbon isotopic compositions (Palot et al., 2012).

We report here the first results of oxygen and carbon isotope analysis of other minerals identified in lower-mantle diamonds (Kaminsky et al., 2009; Wirth et al., 2009) utilizing the NanoSIMS technique.

Samples and analytical method

This study investigated mineral inclusions encapsulated in two diamond grains from the Juina area, Mato Grosso State, Brazil. Both diamonds were extracted from the same prospecting sample #8 collected within the Rio Soriso basin (see Fig. 2 in Kaminsky et al., 2009). These inclusions are daughter minerals, formed as a result of the decomposition of the initial carbonatitic association and form two assemblages: calcite + wollastonite II and calcite + monticellite (Fig. 1). Calcite and wollastonite II were analyzed within a 4×4 μm rhombic-shaped inclusion in diamond #8/103, foil #1734 (Kaminsky et al., 2009). Calcite forms the matrix of the inclusion occurring as a polycrystalline aggregate with individual crystals on the order of 1–2 μm each (Fig. 1a). Its composition is essentially $CaCO_3$ (Ca=99.26 at. % of the cation group), with an admixture of Sr (0.74 at. % of the cation group) and trace quantities of Ba. Such Sr-enriched calcite is considered to be primary magmatic (e.g., Armstrong et al., 2004). Wollastonite II (high) was identified from its diffraction pattern; it occurs along with nyerereite and a Ca-garnet. The wollastonite II forms several near-euhedral grains, 50–500 nm in size. The chemical composition of wollastonite II is (in at. %): Ca=49.7, Si=50.1, and Fe=0.2.

The calcite + monticellite assemblage was studied from diamond #8/104 (foil #1598) (Wirth et al., 2009). This plate-like inclusion, only a few micrometers in length and ca. 200 nm thick, is composed of calcite, that comprises the bulk of the inclusion, and sub-micrometre-sized monticellite, cuspidine, wollastonite II, metallic alloys, amorphous material with a C-Ca-Si-O composition, and minor fluid bubbles, 5–50 nm in size (Fig. 1b). The calcite, as in sample #8/103, is polycrystalline, with an average grain size of approximately 1–2 μm. However, in this sample, the chemical composition of the mineral is that of pure calcite, that may be explained by its recrystallization. Monticellite (identified from its diffraction pattern) has a composition of (at. %): Si=29.8, Fe=11.4, Mg=23.9, and Ca=33.6, with minor admixtures of Al (0.7), Ti (0.3), and Mn (0.3).

Both diamonds belong to the same geological sample, ~0.5 m^3 in size. Both studied mineral assemblages in these diamonds belong to the natrocarbonatite association, in which nyerereite $(Na,K)_2Ca(CO_3)_2$ forms the matrix of the inclusion (Kaminsky et al., 2009, 2015).

The major challenge for isotopic study of these mineral grains was their very small, sub-micrometre, sizes. We performed the analysis of the samples utilizing a NanoSIMS 50 instrument at the Lawrence Livermore National Laboratory, USA. We measured the carbon and oxygen isotope compositions of minerals from the same FIB foils that had previously been examined by TEM at the GeoForschungsZentrum Potsdam, Germany (Fig. 1). Oxygen and carbon isotope abundances were determined using a focused primary 0.3 pA Cs+ beam, ca. 60 nm in diameter, which was rastered over a 4×4 μm^2 area to produce quantitative secondary ion images. Each ion image was subdivided into calcite, silicate and diamond regions (Fig. 2), which were analyzed separately. An electron flood gun was used for charge compensation. Secondary ions were acquired by simultaneously measuring $^{12}C^-$, $^{13}C^-$, $^{16}O^-$, $^{18}O^-$ and $^{28}Si^-$ on electron multipliers at a mass-resolving power of ca. 3600. Isotope ratios were determined with the L'Image software developed by L. Nittler, Carnegie Institution of Washington, DC. One could expect the quasi-simultaneous arrival (QSA) effect on C isotopes (Slodzian et al. 2004). However, in our experiments, no variations of the instrumental fractionation factor with count rates were observed. Further an admixture of Sr (0.74 at. %) and a trace quantity of Ba are not so high as to influence the O isotope composition (Valley and Kita, 2009). Other elemental impurities (Mg, Fe, Mn) in the studied calcites are well below 1 at. %, so the results do not need matrix correction (Rollion-Bard and Marin-Carbonne 2011). Instrumental mass fractionation was assessed from two calcite standards and the UW-2 garnet standard; they cover the 22 % of $\delta^{13}C$ composition range. The external precision on the standards (84 hrs time) was <4‰ for $\delta^{18}O$ and <9‰ for $\delta^{13}C$ (2σ).

Results

The results obtained in our study were very surprising (Table 1). Against the expected mantle values, the $\delta^{18}O$ values for the calcite + wollastonite II assemblage vary from −1.6 to −3.3‰, and for the calcite + monticellite assemblage from +15.0 to +15.4‰SMOW. The $\delta^{13}C$ values for calcite are −2.8‰ in foil #1734 (in association with wollastonite II) and +9.3‰ VPDB in foil #1598 (in association with monticellite). Both carbonate-silicate assemblages are in isotopic equilibrium, having similar $\delta^{18}O$ values for both mineral phases in each sample. At the same time, there are significant differences in the isotopic characteristics between the two samples: Δ=12.1‰ for carbon and Δ =16.6–18.7‰ for oxygen.

Large error values (6.0–6.1‰for carbon and 4.3–8.2‰for oxygen) include not only analytical errors, but (mainly) isotopic inhomogeneity of samples at the nano-scale level, which is well seen in Fig. 2a and b, where isotopic variations in a ~2 μm calcite grain, reflected in counts per second, vary within ~3,000 ct/s for ^{12}C and ~100,000 ct/s for ^{16}O, that significantly exceeds the analytical errors. The isotopic heterogeneity of mantle minerals has been observed at both the centimeter- and micrometer-scale. For example, a study of a single diamond-bearing peridotite xenolith revealed that, within a volume of only 27 cm^3, the variations for nitrogen content, nitrogen aggregation state, carbon and nitrogen isotopic compositions, respectively, cover 64, 75, 15 and 23% of the ranges known for all peridotitic diamonds (Thomassot et al., 2007). Carbon isotope compositional variations within a single diamond crystal reach 10‰ $\delta^{13}C$ and more (Kaminsky and Sobolev, 1985). At the nano-scale the isotopic variations appeared to be even greater. Diamond #8/106 from Rio Soriso was studied for isotopic composition with NanoSIMS analysis at the Center for Advanced Marine Research, Ocean Research Institute at the University of

Tokyo; 15 spot measurements of $\delta^{13}C$ in the diamond were found to vary from −14 to −25‰ VPDB, with an average at −19.40±3.22‰ (Wirth et al. 2007). The isotopic study of $\delta^{15}N$ in other diamond crystals from the Juina area in Brazil, performed with the use of a Cameca IMS ion microprobe at the Department of Terrestrial Magnetism, Carnegie Institution of Washington, USA, produced results with one-sigma value of ±3‰ (D. Araujo, pers. comm.). This means that the 'error values', in fact, are mainly ranges of isotopic heterogeneity for the studied samples. The real analytical errors are less than 0.4–1.7‰ (see Table 1 and Fig. 4); these values include as well, possible isotopic fractionation between coexisting carbonate and silicate phases, which is particularly significant under low, subsolidus temperatures (100–500 °C) during the course of secondary alteration of the minerals (see below).

Discussion and Preliminary Conclusions

In both analyzed samples calcite is the major mineral. Calcite in sample #1734 is enriched in Sr and, partly, in Ba. Such calcite is inferred to be primary-magmatic (e.g. Armstrong et al., 2004), and its $\delta^{13}C$ value (−2.8‰) is close the range typical of mantle values. Its origin may be attributed to the lower mantle. Earlier, in diamond from the Rio Soriso area, calcite was found in a close ('touching') assemblage with walstromite-like $CaSiO_3$, formed after decompressed CaSi-perovskite, which is typical of the lower-mantle association (Brenker et al., 2007). One of the studied samples #8/103, in the same foil #1734, contains small (less than 100 nm), euhedral nano-inclusions of wüstite (Mg#=1.9–15.3) in association with periclase (Mg#=84.9–92.1) (Fig. 7 in Kaminsky et al., 2009). The coexistence of these phases implies their formation under pressures at or greater than 85 GPa and temperatures in excess of 1000 K (Dubrovinsky et al., 2001); i.e., within the lowermost part of the lower mantle. This conclusion is confirmed by the identification, in the same diamond, of the assemblage of iron carbides, Fe_3C, Fe_7C_3 and $Fe_{23}C_6$ with native iron and graphite, which crystallized within a pressure interval of 50–130 GPa and, possibly, have their source in the outer core or within the D" layer of the lowermost part of the mantle (Kaminsky and Wirth, 2011).

The other minerals, found in association with calcite, are stable at much lower pressures and temperatures. Wollastonite forms as a result of the decomposition of CaSi-perovskite, which starts at ca. 15 GPa with the formation of titanite ($CaSi_2O_5$), larnite (Ca_2SiO_4), walstromite ($CaSiO_3$), and then, at ca. 4 GPa, wollastonite ($CaSiO_3$) (Akaogi et al. 2004). Further uplift and resultant decompression to levels where pressures were less than 0.8 GPa initiated a reaction of wollastonite + fluid to form cuspidine + monticellite. This reaction should have occurred at comparatively low pressures because it is known, from experiments exceeding 0.8 GPa and 1450 °C, that monticellite breaks down to merwinite + forsterite (Kushiro and Yoder, 1964). Unfortunately, little is known about the pressure–temperature stability of cuspidine. Cuspidine was reported to occur in calc-silicate xenoliths from the Bushveld Complex, South Africa which had peak pressure–temperature conditions of 0.11–0.24 GPa and >1200 °C (Buick et al., 2000). The formation of cuspidine and monticellite is the latest-stage event during transit of the host diamond. The existing grains of wollastonite-II found as an inclusion in foil #1734 are metastable relics which were preserved in a closed system. After the consumption of fluorine, the formation of cuspidine at the expense of wollastonite stopped, and the present-day mineral assemblage

is observed. The quantity of monticellite within the inclusion was limited by the availability of Al and Mg (Wirth et al. 2009).

Based on the data obtained, the major trends in the behavior of O and C isotopes during the decomposition of the primary lower-mantle mineral association may be preliminarily marked.

The δ^{18}O SMOW values of the studied assemblages, compared with δ^{18}O values of other diamond associations worldwide, are much dispersed, ranging from −3.3 to +15.4‰ (Fig. 3). They exceed not only values for the upper mantle (from +4.7 to +5.9‰, after Valley et al. 1998), but all other analyses of primary mantle minerals. To our knowledge, there are no isotopic characteristics for carbonatitic fluid inclusions in diamond to date. Klein-BenDavid et al. (2010) performed isotopic analyses for C, N, Sr, Nd and Pb from samples of fibrous diamonds, in which diamond matrix predominates. Figure 4 presents the δ^{13}C vs. δ^{18}O values for the investigated diamond inclusion assemblages, and compares these data to those from other mantle minerals and to the modified primary igneous carbonatite box after Srivastava et al. (2005). The samples, in their δ^{13}C – δ^{18}O coordinates, differ significantly from all previously studied kimberlitic and carbonatitic minerals. Two models can be offered to explain this.

The first model (A in Fig. 4) is an independent C and O fractionation for each sample from a single source. Sample #1598 has a very heavy oxygen isotopic composition, which, in other cases, for other mineral inclusions in diamond, has been explained by the involvement of crustal oxygen in the formation of diamond and associated minerals for the eclogitic association, as a result of deep lithospheric slab subduction (e.g., Jacob et al., 1994; Schulze et al., 2003, 2013; Ickert et al., 2013). However, the δ^{13}C value in the same sample contradicts this suggestion: eclogitic-type diamonds are commonly characterized not by heavy, but, quite the reverse, by light carbon isotopic composition, from −10 to −35‰ δ^{13}C VPDB. Only some eclogitic diamonds from New South Wales, Australia record values of −2 to +4‰ VPDB (e.g., Sobolev et al., 1989; Cartigny, 2005). Such great δ^{13}C values as those reported herein for sample #1598 (+9.3 to +15.4‰ VPDB), have no analogues in igneous and metamorphic rocks. The value of δ^{13}C in sample #1734 has another disagreement with known data on the isotopic systematics of diamond: while the δ^{13}C values are within the average mantle range, the δ^{18}O values (−1.6 and −3.3‰ SMOW) lie within a negative area, never before observed in diamond associations or terrestrial magmas (e.g., Criss, 2008). Such values are characteristic of only meteoric waters or metamorphic rocks that have been affected by such waters.

Suggesting a similar origin for both diamonds and their inclusions (belonging to the same geological sample), their C-O isotopic characteristics may be considered as the result of a single process, and belonging to different stages in the decomposition of the primary lower-mantle mineral association. In this case, an alternative model B (Fig. 4) may be suggested. The two samples should be considered as two ultimately differentiated values from an original single source, which had intermediate δ^{13}C and δ^{18}O values lying between the two samples.

The distinct compositions of calcite in the analyzed assemblages support model B. Calcite in sample #1734, associated with wollastonite II, is enriched in Sr and is primary-magmatic (e.g., Armstrong et al., 2004); its δ^{13}C value (−2.8‰) lies within the range typical of mantle values. Calcite in sample #1598,

associated with monticellite, is chemically pure and has a very heavy carbon isotopic composition ($\delta^{13}C$ =+9.3‰). It may be suggested that, during the ascent of diamond to the surface, wollastonite + remaining fluid, encapsulated in diamond, was dissociated into monticellite + cuspidine (see above). Such dissociation occurs at low, subsolidus temperatures (500 to 100 °C).According to the calculations performed by Wilson et al. (2007), the oxygen isotopic fractionation, in a closed kimberlitic system, within the temperature range from 1100 to 100 °C varies from 6 to 10‰. In this case, the $\delta^{18}O$ values change from the average mantle values of +5 ± 6‰to +12 and +16‰ respectively, which agrees with the observed $\delta^{18}O$ values in sample #1598. The unchanged primary mineral association (like in sample #1734) experienced a complementary isotopic effect resulting in a decrease of the $\delta^{18}O$ value.

The entire mineralogical-geochemical history of the inclusions can be envisaged as follows: Initially, within the lower mantle a calcite + CaSi-perovskite + volatile inclusion was encapsulated within diamond, forming a closed micro-system. During the ascent of the host diamond at ca. 15 GPa, CaSi-perovskite decomposed, with the formation of titanite ($CaSi_2O_5$), larnite (Ca_2SiO_4), walstromite ($CaSiO_3$), and then, at 4 GPa, wollastonite ($CaSiO_3$) (Akaogi et al. 2004). During the final ascent at ca. 0.8 GPa, wollastonite, with the participation of the encapsulated fluid, dissociated into monticellite + cuspidine (Kushiro and Yoder, 1964; Wirth et al., 2009). The oxygen isotope fractionation took place mostly during the latest transformations, at low temperatures (500–100 °C).

Some facts remain, however, unexplained. The suggested fractionation trend B (Fig. 4) with±2‰error lies outside of all known isotopic values for kimberlites, kimberlitic carbonates and primary igneous carbonatites (Fig. 4). In this case, the initial isotopic values for C and O in the lower mantle, as determined for the two analyzed samples, may be different to those of existing estimates for the upper mantle. Alternatively, the obtained data can be considered as the result of local fluctuations within a heterogeneous mantle (e.g., Rampone and Hofmann, 2012). Further isotopic studies of lower-mantle minerals will help to explain better these unusual data.

Acknowledgements

This work was partly supported by University of California Lab Fees Research Program Grant 09-LR-05–116946DOBL. Portions of this work were performed under the auspices of the U.S. DOE by Lawrence Livermore National Laboratory under contract DE-AC52-07NA27344.

References

Akaogi M, Yano M, Tejima Y, IijimaM, Kojitani H (2004) High-pressure transitions of diopside and wollastonite: phase equilibria and thermochemistry of $CaMgSi_2O_6$, $CaSiO_3$ and $CaSi_2O_5$–$CaTiSiO_5$ system. Phys Earth Planet Inter 143–144:145–156

Armstrong JP, Wilson MR, Barnett RL, Nowicki T, Kjarsgaard BA (2004) Mineralogy of primary carbonate-bearing hypabyssal kimberlite, Lac de Gras, Slave Province, Northwest Territories, Canada. Lithos 76:415–433

Brenker FE, Vollmer C, Vincze L, Vekemans B, Szymanski A, Janssens K, Szaloki I, Nasdala L, Kaminsky F (2007) Carbonates from the lower part of transition zone or even the lower mantle. Earth Planet Sci Lett 260:1–9

Buick IS, Gibson R, Wallmach T, Metz J (2000) The occurrence of cuspidine, foshagite and hillebrandite in calc-silcate xenoliths from the bushveld complex, South Africa. S Afr J Geol 103:249–254

Cartigny P (2005) Stable isotopes and the origin of diamond. Elements 1: 79–84

Criss RE (2008) Terrestrial oxygen isotope variations and their implications for planetary lithospheres. Rev Mineral Geochem 68:511–526

Deines P, Harris JW, Robinson DN, Gurney JJ, Shee SR (1991) Carbon and oxygen isotope variations in diamond and graphite eclogites from Orapa, Botswana, and the nitrogen content of their diamonds. Geochim Cosmochim Acta 55:515–524

Dubrovinsky LS, DubrovinskaiaNA, Annersten H, Halenius E, Harryson H (2001) Stability of $(Mg_{0.5}Fe_{0.5})O$ and $(Mg_{0.8}Fe_{0.2})O$ magnesiowüstites in the lower mantle. Eur J Mineral 13:857–861

Giuliani A, Phillips D, Kamenetsky VS, Fiorentini ML, Farquhar J, Kendrick MA (2014) Stable isotope (C, O, S) compositions of volatile-rich minerals in kimberlites: a review. Chem Geol 374–375:61–83

Harte B (2010) Diamond formation in the deep mantle: the record of mineral inclusions and their distribution in relation to mantle dehydration zones. Mineral Mag 74:189–215

Harte B, Hudson NFC (2013) Mineral associations in diamonds from the lowermost upper mantle and uppermost lower mantle. Spec Issue J Geol Soc India 1:235–254, Proceedings of the 10th International Kimberlite Conference, Vol. 1

Harte B, Harris JW, Hutchison MT,Watt GR,Wilding MC (1999) Lower mantle mineral associations in diamonds from Sao Luiz, Brazil. In: Fei Y, Bertka CM, Mysen BO (eds), Mantle petrology: field observations and high pressure experimentation: a tribute to Francis R. (Joe) Boyd. Geochem Soc Spec Publ 6: 125–153

Ickert RB, Stachel T, Stern RA, Harris JW (2013) Diamond from recycled crustal carbon documented by coupled $\delta^{18}O$- $\delta^{13}C$ measurements of diamonds and their inclusions. Earth Planet Inter 364:85–97

Jacob D, Jagoutz E, Lowry D, Mattey D, Kudrjavtseva G (1994) Diamondiferous eclogites from Siberia: remnants of archean oceanic crust. Geochim Cosmochim Acta 58:5191–5207

Jacob D, Jagoutz E, Lowry D, Zinngrebe E (1998) Comment on ‘the origins of Yakutian Eclogite Xenoliths’ by Snyder GA et al. J Petrol 39:1527–1533

Kaminsky FV (2012) Mineralogy of the lower mantle: a review of ‘superdeep’ mineral inclusions in diamond. Earth Sci Rev 110:127–147

Kaminsky FV, Sobolev NV (1985) Variations in carbon isotope composition within diamond crystals. Dokl Akad Nauk SSSR 285:1436–1439 (in Russian)

Kaminsky FV, Wirth R (2011) Iron carbide inclusions in lower-mantle diamond from Juina, Brazil. Can Mineral 49:555–572

Kaminsky F, Wirth R, Matsyuk S, Schreiber A, Thomas R (2009) Nyerereite and nahcolite inclusions in diamond: evidence for lower-mantle carbonatitic magmas. Mineral Mag 73:797–816

Kaminsky FV, Ryabchikov ID, Wirth R (2015) A primary natrocarbonatitic association in the deep earth. Mineral Petrol. doi:10.1007/s00710-015-0368-4

Klein-BenDavid O, Pearson DG, Nowell GM, Ottley C, McNeill JCR, Cartigny P (2010) Mixed fluid sources involved in diamond growth constrained by Sr–Nd–Pb–C–N isotopes and trace elements. Earth Planet Sci Lett 289:123–133

Kostrovitskii SI, Solov'eva LV, Gornova MA, Alymova NV, Yakovlev DA, Ignat'ev AV, Velivetskaya TA, Suvorova LF (2012) Oxygen isotope composition in minerals of mantle parageneses from Yakutian kimberlites. Transact (Dokl) Russ Acad Sci/Earth Sci Sect 444:579–584

Kushiro I, Yoder HS (1964) Breakdown ofmonticellite and akermanite at high pressures. Year B Carnegie Inst Wash 63:81–83

Lowry D, Mattey DP, Harris JW (1999) Oxygen isotope composition of syngenetic inclusions in diamond from the Finsch Mine, RSA. Geochim Cosmochim Acta 63:1825–1836

Mattey D, Lowry D, MacPherson C (1994) Oxygen isotope composition of mantle peridotite. Earth Planet Sci Lett 128:231–241

Page FZ, Bin Fu B, Kita NT, Fournelle J, Spicuzza MJ, Schulze DJ, Viljoen F, Basei MAS, Valley JW (2007) Zircons from kimberlite: New insights from oxygen isotopes, trace elements, and Ti in zircon thermometry. Geochim Cosmochim Acta 71:3887–3903

Palot MP, Cartigny P, Harris JW, Kaminsky FV, Stachel T (2012) Evidence for deep mantle convection and primordial heterogeneity from N and C stable isotopes in diamond. Earth Planet Sci Lett 357–358:179–193

Rampone E, Hofmann AW (2012) A global overview of isotopic heterogeneities in the oceanic mantle. Lithos 148:247–261

Rollion-Bard C,Marin-Carbonne J (2011) Determination of SIMS matrix effects on oxygen isotopic compositions in carbonates. J Analyt Atom Spectrom 26:1285–128

Schulze DJ, Harte B, Valley JW, Brenan JM, Channer DMDR (2003) Extreme crustal oxygen isotope signatures preserved in coesite in diamond. Nature 423:68–70

Schulze D, Harte B, Page FZ, Valley JW, Channer DMDR, Jaques AL (2013) Anticorrelation between low $\delta^{13}C$ of eclogitic diamonds and high $\delta^{18}O$ of their coesite and garnet inclusions requires a subduction origin. Geology 41:455–458

Slodzian G, Hillion F, Stadermann FJ, Zinner E (2004) QSA influences on isotopic ratio measurements. Appl Surf Sci 231–232:874–877

Snyder GA, Taylor LA, Jerde EA, Clayton RN, Mayedo TK, Deines P, Rossman GR, Sobolev NV (1995) Archean mantle heterogeneity and the origin of diamondiferous eclogites, Siberia: evidence from stable isotopes and hydroxyl in garnet. Am Mineral 80:799–809

Sobolev NV, Galimov EM, Smith CB, Yefimova ES, Maltsev KA, Hall EE, Usova LV (1989) Morphology, inclusions and carbon isotopic composition of diamonds from the King George alluvial deposit and the Argyle lamproitic pipe, Western Australia. Russ Geol Geophys 12:3–18

Spetsius ZV, Griffin WL, Taylor LA, O'Reilly SY, Mityukhin SI, Valley JW, Spicuzza M (2008) Trace elements and oxygen isotopes in garnets from diamondiferous xenoliths, Nurbinskaya pipe, Yakutia: implications for diamond genesis. 9th International Kimberlite Conference, Frankfurt (No. 9IKC-A-00140)

Srivastava RK, Heaman LM, Sinha AK, Shihua S (2005) Emplacement age and isotope geochemistry of Sung Valley alkaline–carbonatite complex, Shillong Plateau, northeastern India: Implications for primary carbonate melt and genesis of the associated silicate rocks. Lithos 81:33–54

Tappe S, Foley SF, Kjarsgaard BA, Romer RL, Heaman LM, Stracke A, Jenner GA (2008) Between carbonatite and lamproite – diamondiferous torngat ultramafic lamprophyres formed by carbonate-fluxed melting of cratonic MARID-type metasomes. Geochim Cosmochim Acta 72:3258–3286

Thomassot E, Cartigny P, Harris JW, Vilhoen KS (2007) Methane-related diamond crystallization in the Earth's mantle: stable isotope evidences from a single diamond-bearing xenoliths. Earth Planet Sci Lett 257:362–371

Valley JW, Kita NT (2009) In situ oxygen isotope geochemistry by ion microprobe, In: Fayek M (ed) MAC short course: secondary ion mass spectrometry in the earth sciences, 41: 19–63

Valley JW, Kinny PD, Schulze DJ, Spicuzza MJ (1998) Zircon megacrysts from kimberlite: oxygen isotope variability among mantle melts. Contrib Mineral Petrol 133:1–11

Viljoen KS, Schulze DG, Quadling AG (2005) Contrasting group I and group II eclogite xenolith petrogenesis: Petrological, trace element and isotopic evidence from eclogite, garnet-websterite and alkremite xenoliths in the kaalvallei kimberlite, South Africa. J Petrol 46:2059–2090

Wang Z, Bucholz C, Skinner B, Shimizu N, Eiler J (2011) Oxygen isotope constraints on the origin of high-Cr garnets from kimberlites. Earth Planet Sci Lett 312:337–347

Wilson MR, Kjarsgaard BA, Taylor B (2007) Stable isotope composition of magmatic and deuteric carbonate phases in hypabyssal kimberlite, Lac de Gras field, Northwest Territories, Canada. Chem Geol 242:435–454

Wirth R, Pinti D, Sano Y, Takahata N, Kaminsky F (2007) Indications of crustal carbon in lower-mantle Juina diamond as revealed by FIB/TEM and NanoSIMS investigations. AGU Fall Meeting, San Francisco, Abstract

Wirth R, Kaminsky F, Matsyuk S, Schreiber A (2009) Unusual micro and nano-inclusions in diamonds from the Juina Area, Brazil. Earth Planet Sci Lett 286:292–303

Figure Captions

Figure 1. HAADF TEM images of the studied associations: a) calcite (Cc) + wollastonite (Wo II) association from inclusion in diamond #8/103, foil #1734; b) calcite (Cc) + monticellite + wollastonite (wo) + cuspidine (Cus) association from inclusion in diamond #8/104, foil #1598. The bright spots in diamond indicated by white arrows are native iron (left) and iron + manganese (right).

Figure 2. Ion images of the isotopic ratios of ^{12}C, ^{16}O and ^{28}Si in sample #8/104 (foil #1598). White (black for ^{18}O) lines outline the counted areas of the mineral grains. Dia – diamond, Cal – calcite, Mtc – monticellite. Color bars indicate yield of ions (intensity of response) in counts per one second (ct/s). The scales are set by the image processing software

Figure 3. Values of $\delta^{18}O$ for mantle minerals of diamond facies. Analyses of ultramafic association minerals after Mattey et al. (1994); Lowry et al. (1999); Spetsius et al. (2008); analyses of eclogitic association minerals after Deines et al. (1991); Jacob et al. (1994, 1998); Snyder et al. (1995); Lowry et al. (1999); Schulze et al. (2003, 2013); Viljoen et al. (2005); Spetsius et al. (2008); Ickert et al. (2013). Analyses of zircon from kimberlites after Valley et al. (1998) and Page et al. (2007). Number of analyses is shown in brackets at mineral names: Ol – olivine, Opx – orthopyroxene, Cpx – clinopyroxene, Grt – garnet, Coe – coesite, Cal – calcite, WoII – wollastonite II, CaSiPrv – CaSi-perovskite, Mtc – monticellite. Data on lower-mantle CaSi-perovskite from Harte et al. (1999). Shaded area is the “garnet mantle region” after Valley et al. (1998).

Figure 4. Isotopic composition of oxygen and carbon in lower mantle minerals. Modified primary igneous carbonatite (PIC) box (red) after Srivastava et al. (2005); the field of carbonatites worldwide after Tappe et al. (2008); the upper-mantle $\delta^{18}O$ area after Valley et al. (1998); the upper-mantle $\delta^{13}C$ area after Cartigny (2005). Field of primary carbonates in kimberlites after Wilson et al. (2007). Explanations in text.

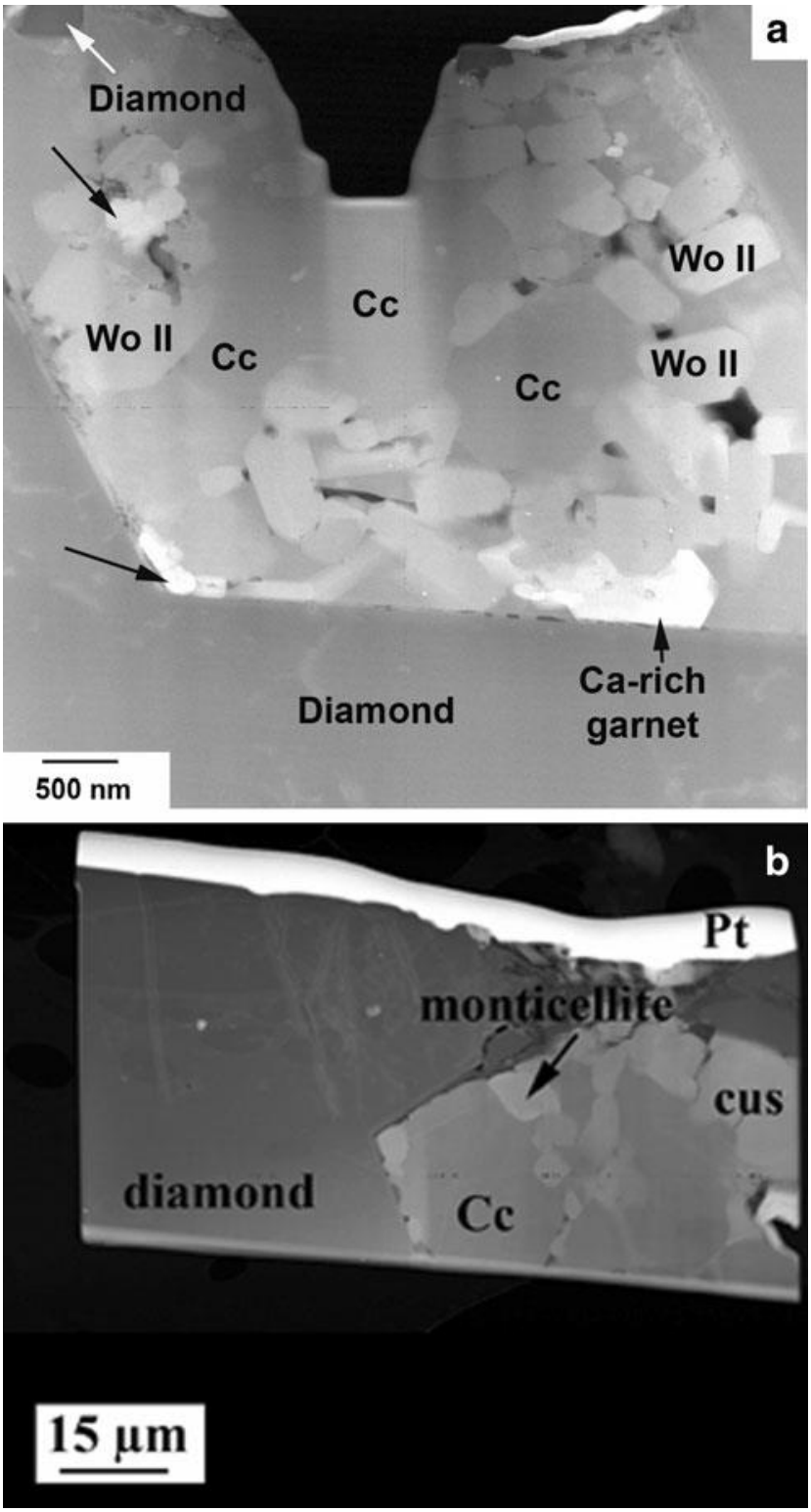
a
Diamond
Wo II
Cc
Wo II
Cc
Cc
Wo II
Ca-rich
garnet
Diamond
500 nm
b
Pt
monticellite
cus
diamond
Cc
15 µm

Figure 1.

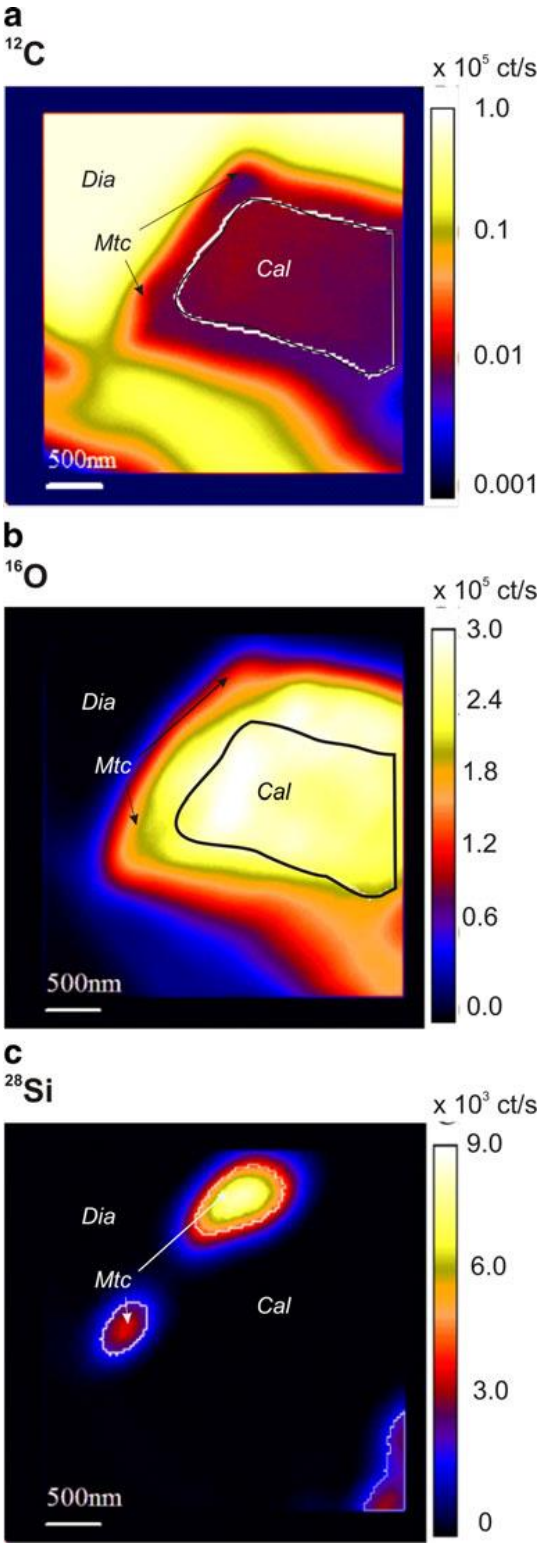
a
^{12}C
x 10^5 ct/s
1.0
0.1
0.01
0.001
Dia
Mtc
Cal
500nm
b
^{16}O
x 10^5 ct/s
3.0
2.4
1.8
1.2
0.6
0.0
Dia
Mtc
Cal
500nm
c
^{28}Si
x 10^3 ct/s
9.0
6.0
3.0
0
Dia
Mtc
Cal
500nm

Figure 2.

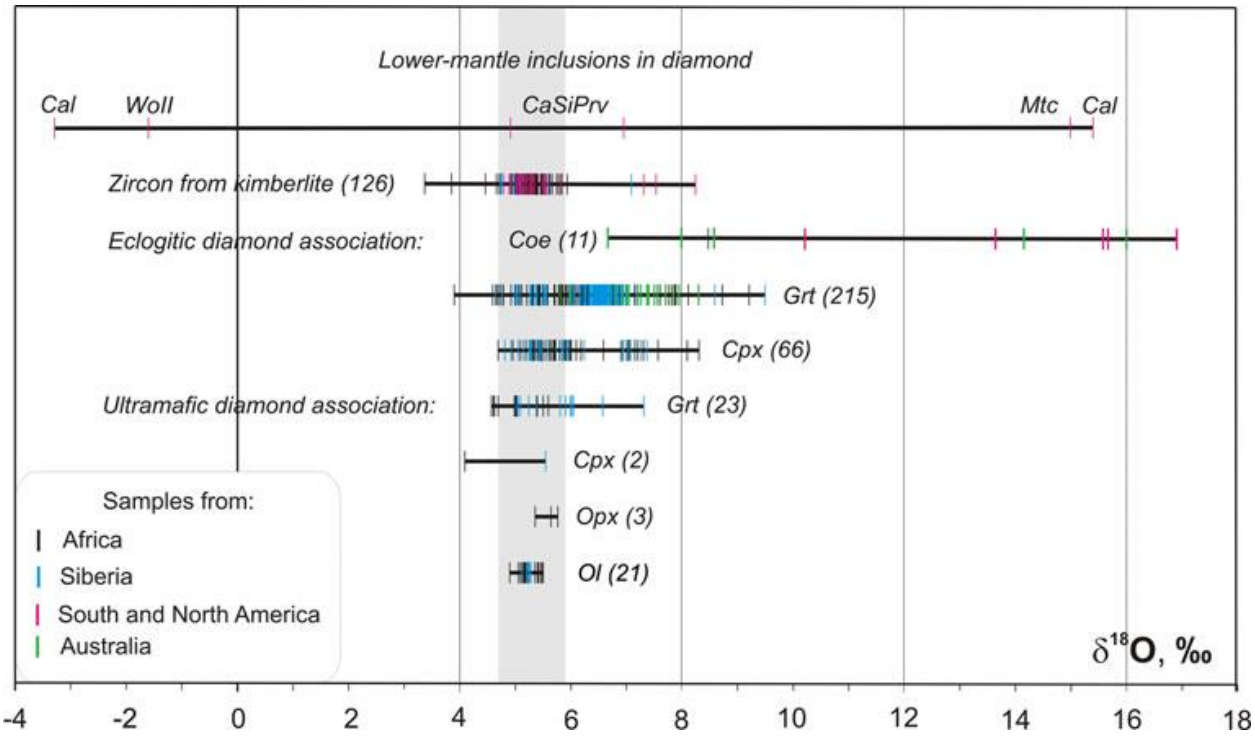
Lower-mantle inclusions in diamond
Cal
WolI
CaSiPrv
Mtc
Cal
Zircon from kimberlite (126)
Eclogitic diamond association:
Coe (11)
Grt (215)
Cpx (66)
Ultramafic diamond association:
Grt (23)
Cpx (2)
Opx (3)
Ol (21)
Samples from:
Africa
Siberia
South and North America
Australia
δ18O, ‰
-4
-2
0
2
4
6
8
10
12
14
16
18

Figure 3.

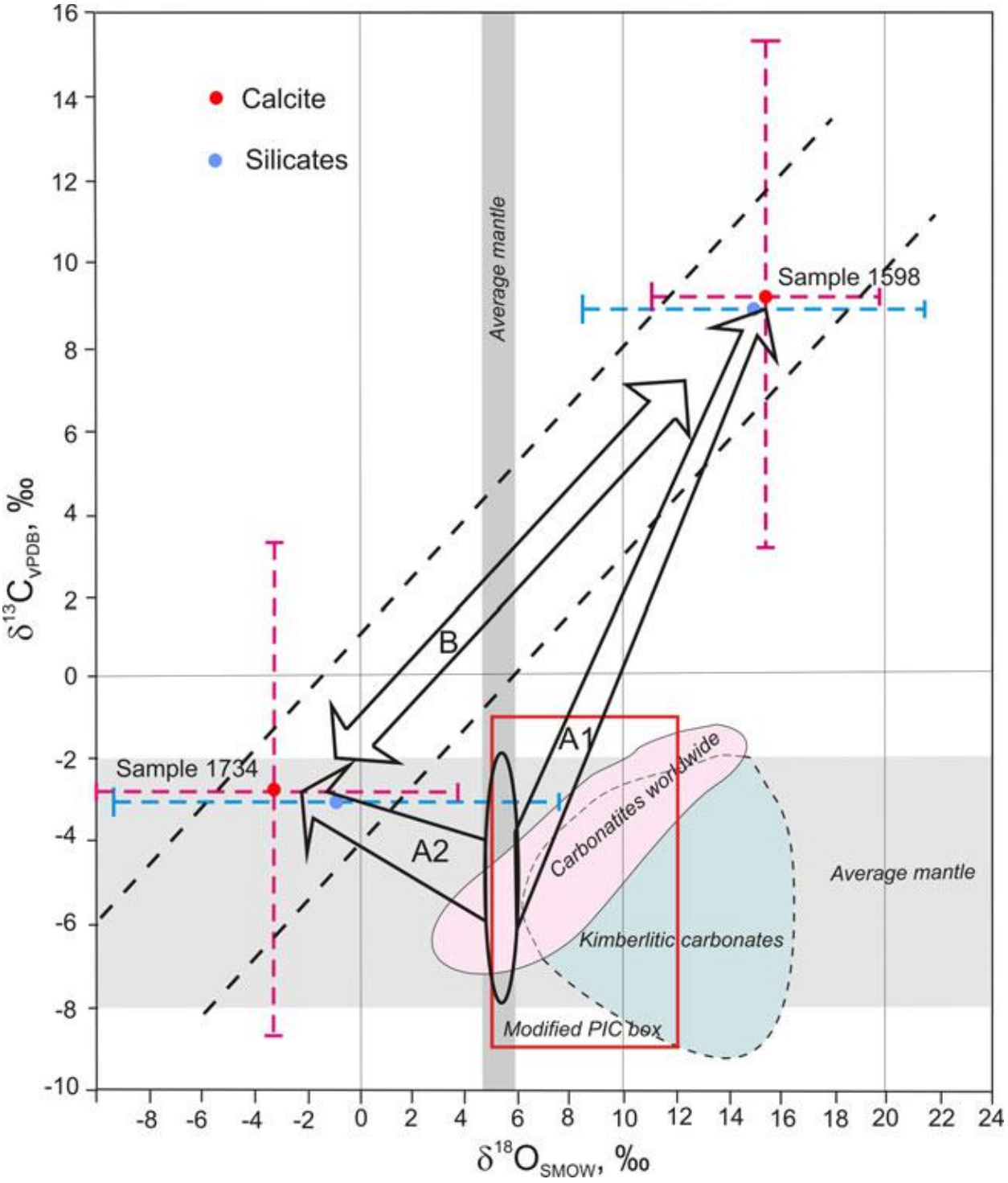
Calcite
Silicates
Average mantle
Sample 1598
Sample 1734
B
A1
A2
Carbonatites worldwide
Kimberlitic carbonates
Modified PIC box
Average mantle
$\delta^{13}C_{VPDB}$, ‰
$\delta^{18}O_{SMOW}$, ‰

Figure 4.

Table 1. Values of $\delta^{18}O$ and $\delta^{13}C$ in carbonate and silicate inclusions.

Sample, mineral	**$\delta^{18}O \pm 1\sigma$,‰ SMOW**	**$\delta^{13}C \pm 1\sigma$,‰ VPDB**
Foil #1734		
Calcite	-3.3±7.0	-2.8±6.0
Wollastonite	-1.6±8.2	
Foil #1598		
Calcite	+15.4±4.3	+9.3±6.1
Monticellite	+15.0±6.5	